



POLITECNICO
MILANO 1863

DEPARTMENT OF INDUSTRIAL AND INFORMATION ENGINEERING
MASTER OF SCIENCE IN SPACE ENGINEERING

**INTERPLANETARY AND PLANETARY
EXPLORER MISSION**

Professor:
Prof. Colombo Camilla

Group ID:
2341
Students:
Barbiera Andrea
De Luca Leo
Perusini Gianluca
Poverini Viola

Table of contents

1 Interplanetary Mission	2
1.1 Introduction	2
1.2 Design process	2
1.2.1 Constraints	2
1.2.2 Assumptions	2
1.2.3 Preliminary estimations	3
1.2.4 Solution method	3
1.3 Final solution	5
1.3.1 Heliocentric trajectory	5
1.3.2 Flyby: powered gravity assist manoeuvre	6
1.4 Discussion	7
1.5 Conclusions	7
References	8
2 Planetary Explorer Mission	9
2.1 Introduction	9
2.2 Nominal orbit	9
2.3 Ground-track	9
2.4 Orbit propagation with perturbations	10
2.5 History of the Keplerian elements and Filtering of high frequencies . . .	11
2.6 Orbit plot	13
2.7 Comparison with real data	14
2.8 Conclusions	14
References	14

1 Interplanetary Mission

1.1 Introduction

This report aims to present the preliminary mission analysis for the PoliMi Space Agency's 'interplanetary explorer mission' which is set to depart from Saturn and visit Asteroid N.59 ("ephNEO" notation) with an intermediate powered gravity assist (flyby) around Jupiter. The focus of this study is to find and characterize the optimal transfer orbits to minimize the cost of the mission (ΔV).

1.2 Design process

1.2.1 Constraints

To satisfy the main mission requirements, the constraints shown in Table 1 must be considered.

Departure	Flyby	Flyby Minimum Altitude [km]	Arrival	Earliest Departure	Latest Arrival
Saturn	Jupiter	5000	Asteroid N.59	01/01/2028 00:00	01/01/2058 00:00

Table 1: Mission Requirements.

1.2.2 Assumptions

To carry out the mission, the patched conic method has been used. Doing so, the following assumptions [1] have been made:

- The initial heliocentric orbit is equal to that of Saturn;
- The final heliocentric orbit is equal to that of Asteroid N.59;
- All manoeuvres are assumed to be instantaneous;
- Possible encounters with other celestial bodies and perturbations are ignored;
- The sphere of influence (SOI) of each planet in the heliocentric frame is neglected;
- The SOI of each planet in their planetocentric frame is supposed to be infinite;
- Flyby time is negligible, with supposed uniform gravitational field around the planet.

In particular, the last three assumptions are evaluated in the discussion paragraph to see if they can be applied to the interplanetary mission.

1.2.3 Preliminary estimations

The time windows for each transfer leg were tailored to the goals and characteristics of the mission. Narrowing down the range of possible dates allows to reduce the required computational effort and avoids the selection of unreasonable combinations. Some of the orbital parameters of the celestial bodies involved are shown in Table 2. They were calculated using the provided functions.

Celestial body	Semi-major axis [km]	Eccentricity	Inclination [deg]
Saturn	1.4294e9	0.0554	2,4873
Jupiter	7.7829e8	0.0486	1.3006
Asteroid N.59	3.5156e8	0.7265	25.1430

Table 2: Orbit characteristics for all three celestial bodies.

From the values shown in Table 2 it can be observed that Saturn and Jupiter have nearly circular orbits with very small relative inclinations (coplanar). An Hohmann transfer was therefore considered as an ideal first leg since it is known to be the most efficient transfer in this case [4]. A general Hohmann transfer between these two bodies was found to have a transfer period of 9.5 years. To avoid missing any Hohmann-like transfers that would result in a lower ΔV overall, a margin of 3 years was applied to the previously mentioned value which is about $\pm 15\%$ of the Hohmann TOF.

1.2.4 Solution method

Following the consideration mentioned above, the focus shifted to the second interplanetary leg. Table 2 shows that the asteroid's orbit is characterized by greater eccentricities and inclinations than those of the two gas planets. Because of these differences, as well as the fact that a proper synodic period between the 3 celestial bodies could not be defined within the required time windows, an evaluation of the transfers' duration was completed to reduce the width of the time windows. In fact, TsynSJ is almost 20 years and TsynJA is a little more than 5 years. By doing so, the flyby and arrival windows were reduced to 20 years (2036-2056 and 2038-2058, respectively) with bimonthly discretization. At this stage, the most promising regions for the second transfer were identified through an analysis of the ΔV required to enter the asteroid's orbit (Figure 1.a). In this analysis, we tried to reduce the computational effort of the grid search through constraints on TOFs, as they must be greater than TPAR and less than Jupiter's orbital period. After completing this, the first leg and the flyby were added to the analysis. Now, the grid search is over the 3 DoFs using three nested loops. Once again, additional constraints such as energy constraints, minimum altitude of the flyby, and similarity of the first ToF and ToFH of $\pm 15\%$,

were considered to refine the options. These additional steps led to the identification of four promising time windows (Figure 1.b).

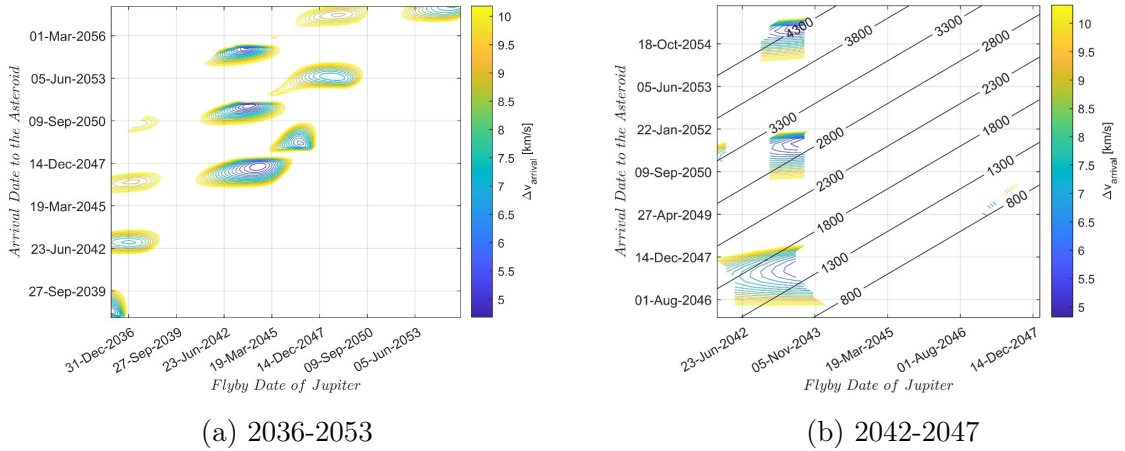


Figure 1: Arrival Cost Plot.

For each of the regions, an individual study was conducted with variable discretization and amplitude on the departure window but fixed discretization and ± 2 months amplitude on the flyby and arrival ones. The results of this analysis can be seen in the MATLAB folder “CodeAssignment1Analysis”. This led to the identification of the final best solution.

A contour plot analysis of the first leg is of little significance since, in addition to assuming a Hohmann manoeuvre, the first cruise transfer is characterized by a repetitiveness that cannot be seen in the given windows. The Cost Plot referring to the first interplanetary leg is given in the conclusions. The ladder is characterized by larger time windows that allows to note the repetitiveness characterizing the Cost Plots.

Having chosen the favourable case, the solution was refined using a gradient-based optimizer provided by the MATLAB function *fminunc.m*. The initial guess of the minimum value required by the command was set as the value obtained from the previous analysis. With the three-time instants, the interplanetary travel was fully defined.

Lastly, an analysis on large time windows was performed with a discretization related to the periods of the celestial bodies to avoid excessive computational effort. The results of this analysis correspond exactly with the previous findings; therefore, the assumption of a quasi-Hohmann transfer for the first interplanetary leg was further validated.

1.3 Final solution

At this stage, the parameters characterizing the interplanetary mission are shown in Table 3. The **total ΔV** is **7.8658 km/s** while the **total ToF** is **almost 14 years**.

Stage	ΔV	Time
Departure ($1_{st} Leg$)	1.9358	08/08/2033 - 03:35
Flyby	0.5872	29/07/2043 - 06:11
Arrival ($2_{nd} Leg$)	5.3427	31/07/2047 - 00:04

Table 3: Orbit characteristics for all three celestial bodies.

1.3.1 Heliocentric trajectory

Table 4 and 5 shows the parameters characterizing the two interplanetary legs.

Parameters	a [km]	e [-]	i [deg]	Ω [deg]	ω [deg]
1st Transfer Leg	1.0675e+09	0.2766	1.7700	265.2627	29.1110
2nd Transfer Leg	5.6523e+08	0.5363	24.8801	92.3157	24.2365

Table 4: Parameters characterizing the two interplanetary legs.

Parameters	θ_i [deg]	θ_f [deg]
1st Transfer Leg	167.7134	337.5065
2nd Transfer Leg	155.2789	247.8959

Table 5: Parameters characterizing the two interplanetary legs.

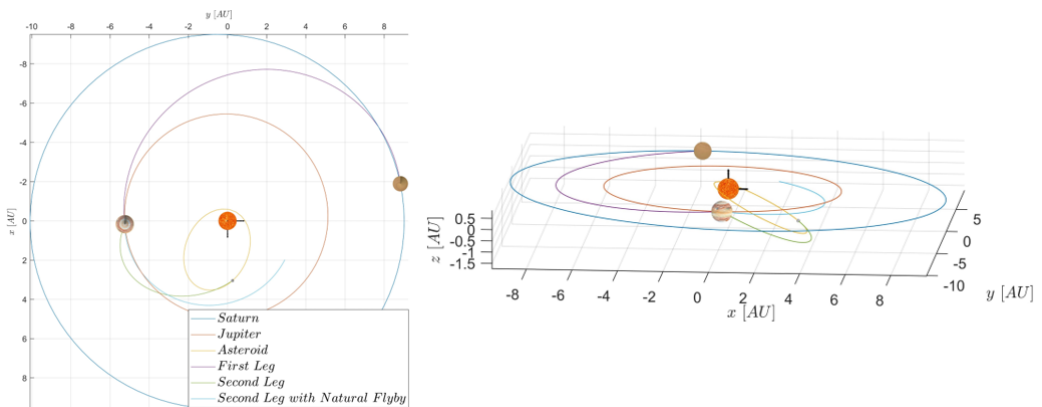


Figure 2: Interplanetary trajectory.

In Figure 2 is displayed the optimal interplanetary trajectory and the second leg subsequent to a natural flyby. The characteristic shape of a Hohmann-like transfer can be visually appreciated. Furthermore, the flyby of Jupiter represents the Descending Node of the Second Leg, allowing the required plane change manoeuvre to be performed with less propellant consumption.

1.3.2 Flyby: powered gravity assist manoeuvre

The plane-change manoeuvre is known to be very expensive [1]. For this reason, the flyby of Jupiter allows to make a plane change more economically, saving a considerable amount of propellant. Thanks to Jupiter's powerful gravitational field, a large change in heliocentric velocities can be achieved at the price of a small manoeuvre at the pericentre of the hyperbola. In fact, the ratio of velocity variation obtained at the extremes of the SOI to the required manoeuvre at the pericentre is 15.6556. This is a very large value and reaffirms the importance that flybys, especially of Jupiter, have held in space exploration. This concept will be shown in more detail in the discussion paragraph. The incoming and outgoing hyperbolic trajectories are characterized by the parameters reported in Table 6. The altitude of the pericentre is 63276 km equivalent to 0.905 of Jupiter's radius.

Hyperbola	$v_p [km/s]$	$v_{inf} [km/s]$	e [-]	a [km]	ToF [days]
Incoming	43.6620	$[1.6144; 0.6654; 0.7346]^T$	1.0038	$3.5307e+07$	137.96
Outgoing	44.2492	$[-4.3226; -4.8465; -3.6107]^T$	1.0580	$2.2951e+06$	65.22

Table 6: Characterization of hyperbolic trajectories.

The hyperbolic trajectories are represented in Figure 3. The total duration of the fly-by, considering a finite SOI is: **ΔT=203.1844 days**

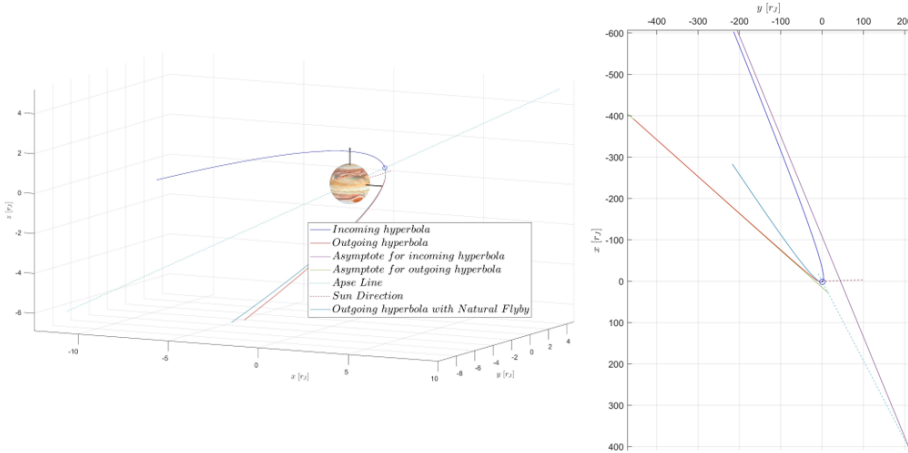


Figure 3: Flyby trajectory.

1.4 Discussion

The given mission characteristics do not exactly meet the assumptions of a Hohmann Transfer; it was therefore necessary to verify it by studying a less constrained case at the level of possible ToFs. To limit the computational effort, it was opted to implement a different discretization for the three bodies and relating it to their orbital periods. This method revealed only one new region in addition to the previously highlighted ones. However, a study of this region characterized by a TOF of the first leg less than the others, revealed a Total ΔV much greater than the others. Therefore, the assumption on the use of a Hohmann transfer was further confirmed. The results of this analysis can be seen in the MATLAB folder “CodeAssignment1Analysis”. Moreover, the ToF of the first leg deviates by only 158 days from an ideal Hohmann, and this corresponds to about 4 of the ToF itself. This value is comparable with the ToF that the spacecraft spends within the SOI and which in the patched conics method is considered as instantaneous, when viewed in the heliocentric frame. Regarding the Jupiter SOI, it can be seen how the hypotheses reported in the assumptions paragraph are verified. In fact, the radius of the SOI is about 690 times the radius of Jupiter and about 6% of the planet’s orbital radius. The power of Jupiter’s gravitational field is well represented by the relationship between the delta velocity obtained at the boundaries of its SOI and the manoeuvring required at the pericentre of the hyperbola (flyby paragraph). This hints at the importance that Jupiter has played and will continue to play in space exploration, enabling travel to the outer belt of the solar system. An example of this can be found in the Pioneer 10 (1973) and Voyager 1 (1979) missions by NASA.

1.5 Conclusions

This report explores the methods used to select an optimal transfer from Saturn to the Asteroid N.59 via a gravity assist manoeuvre around Jupiter. The optimal solution was found to be:

- Departure: 08/08/2033 - 03:35 with a ΔV of 1.9358 km/s;
- Flyby: 29/07/2043 - 06:11 with a ΔV 0.5872 km/s;
- Arrival: 31/07/2047 - 00:04 with a ΔV 5.3427 km/s;
- Altitude of the pericentre of the flyby: 63276 km;
- Comparison of the total velocity change due to the flyby Δv_{fb} with the cost of the powered manoeuvre at pericentre Δv_{ga} : 15.6556 km/s;
- ToF inside the SOI: 203.1844 days;

In particular, the importance of the flyby of Jupiter was highlighted. The planet is capable, at the cost of a meager maneuver, of considerably changing the orbital pa-

rameters of the spacecraft. Although the results may failed to represent the repetition of the Cost Plots based on the Synodic periods, Figure 4 shows the Cost Plot of the first Leg. This plot was not shown previously because, given the relatively small time windows of the assignment, it was not possible to capture this phenomenon. With two 120-year windows and nearly co-planar and circular orbits (Saturn and Jupiter), the pattern of repetitions becomes clear.

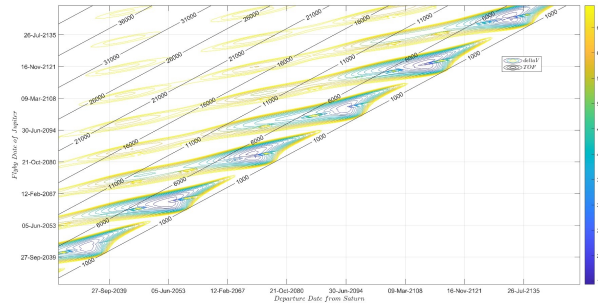


Figure 4: Repetition pattern based on the Synodic Period.

The assumptions made were verified and validated when possible. The computational effort was decreased considerably compared to a coarse and rough approach concerned with window completeness. The results obtained are satisfactory and feasible at today's level of technology, making this mission in fact possible. A further analysis to reduce the $\Delta V_{arrival}$, which is much greater than the other two, could be completed by exploiting resonant flybys and deep-space manoeuvres. Both solutions have already been used and have been proven to significantly improve the trajectory optimization; they should therefore be considered for a more detailed study [2] [3].

References

- [1] Howard D. Curtis, Orbital Mechanics for Engineering Students, Elsevier, 2005.
- [2] Olympio JT, Marmorat JP, Izzo D., Global trajectory optimisation: can we prune the solution space when considering deep space maneuvers?, ARIADNA study, 2007 Sep 10, 6:4101.
- [3] Navagh, John, Optimizing Interplanetary Trajectories with Deep Space Maneuvers, NASA Contractor Report, George Washington University, Hampton, VA, United States, September 1, 1993.
- [4] Menzio, D., 2020, Grid-search applications for trajectory design in presence of flyby.

2 Planetary Explorer Mission

2.1 Introduction

This report aims to present the orbit analysis and ground track estimation for the Polimi Space Agency’s “Planet Explorer Mission” for Earth observation. A study of the J2 and Moon perturbation effects on the ground tracks and orbital elements was also conducted, in which different propagation methods were compared. Lastly, data from an existing object was used to corroborate the results from the model developed.

2.2 Nominal orbit

a [km]	e [-]	i [deg]	Ω [deg]	ω [deg]	θ	ha [km]	hp [km]	m	k
39689	0.8264	21.8645	180	90	0	66109.8	511.8	5	6

Table 7: Nominal orbit.

Table 7 shows that the altitude of perigee is less than 1000 km and the altitude of apogee is greater than 35756 km it is therefore a HEO (highly elliptical orbit). Since the argument of pericentre was chosen to be of 90 degrees the perigee will be in the northern hemisphere.

2.3 Ground-track

The ground-track has been plotted over 3 different times relevant for both the nominal and the repeating orbits: one period, twelve periods (in order to cover all the longitudes in the range of $[-i; +i]$ of latitude) and three months (in order to see all the effects of perturbations).

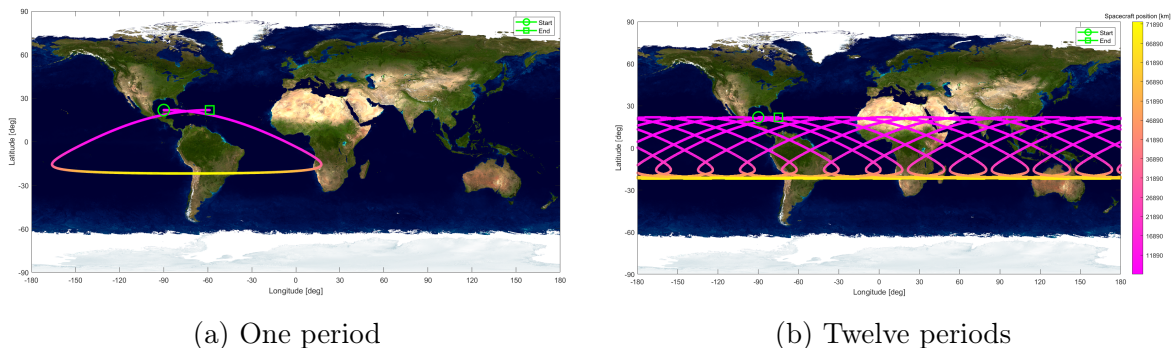


Figure 5: Ground-tracks of the Unperturbed Nominal orbit over two different times

In order to have a repeating ground-track with a ratio of 6:5 it is necessary to calculate the modified semi-major axis (a_r) using the following Equation (1):

$$a_r = \sqrt[3]{\mu_E} \left(\frac{m}{\omega_E \cdot k} \right)^2 = 37340.199 \text{ km} \quad (1)$$

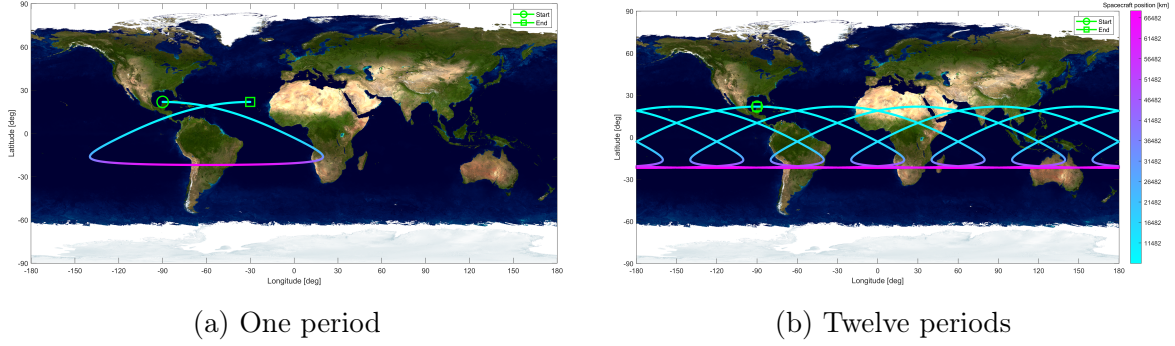


Figure 6: Ground-tracks of the Unperturbed Repeating orbit over two different times

Adding the perturbations (J2+Moon), it's possible to plot both the ground-tracks of the unperturbed and perturbed orbits (for both the nominal and the repeating orbits) to make a comparison.

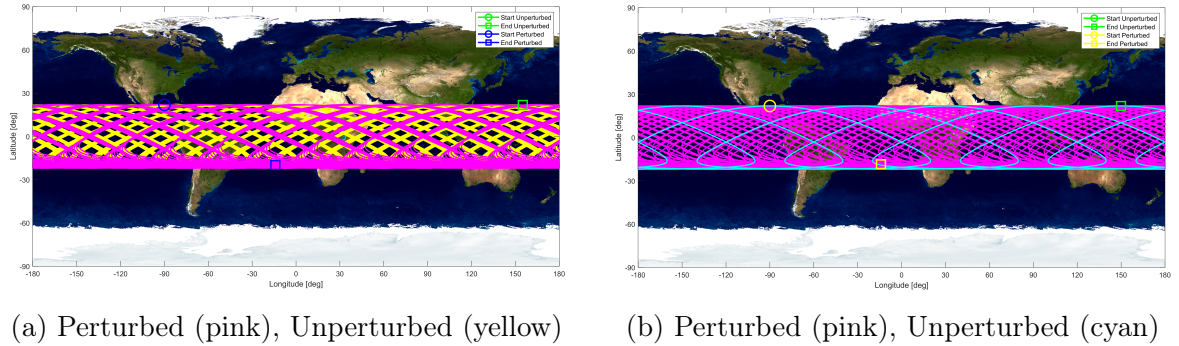


Figure 7: Ground-tracks of the Perturbed and Unperturbed nominal (left) and repeating (right) orbits over three months

Figure 7 shows that the repeating ground-track does not work under the presence of perturbations because orbital elements change due to the presence of J2+Moon perturbations.

2.4 Orbit propagation with perturbations

Integrating in Cartesian coordinates for approximately six months (202 periods) took about forty-two seconds, while using Gauss's planetary equations [1] took about thirty-nine seconds.

2.5 History of the Keplerian elements and Filtering of high frequencies

The principal secular effect of J2 is a change over time of the Right ascension of the ascending node, the argument of pericentre and the true anomaly. Since the inclination of the orbit is between 0-90 deg, the change of the RAAN causes a nodal regression in the west-word direction. On the other hand, the change of the Argument of Pericentre causes a perigee precession (apse line rotation). The principal secular effect of the Third body perturbation of the Moon is a change over time of the inclination, eccentricity and argument of pericentre. From the numerical integration it can be observed that, in addition to the changes in all the previous orbital elements, there is also a variation in the semi-major axis.

The following figures show the evolution of the Keplerian elements over 6 month (approximately 202 orbital periods) and the relative error between the propagation using the Gauss's planetary equations and the one using Cartesian coordinates. To plot the change in the orbital elements starting from the results of the integration in Cartesian coordinates it's necessary to convert the position and velocity vectors in Keplerian orbital elements and it took about fifteen seconds (that added to the forty-two seconds of propagation leading to a total of approximately one minute).

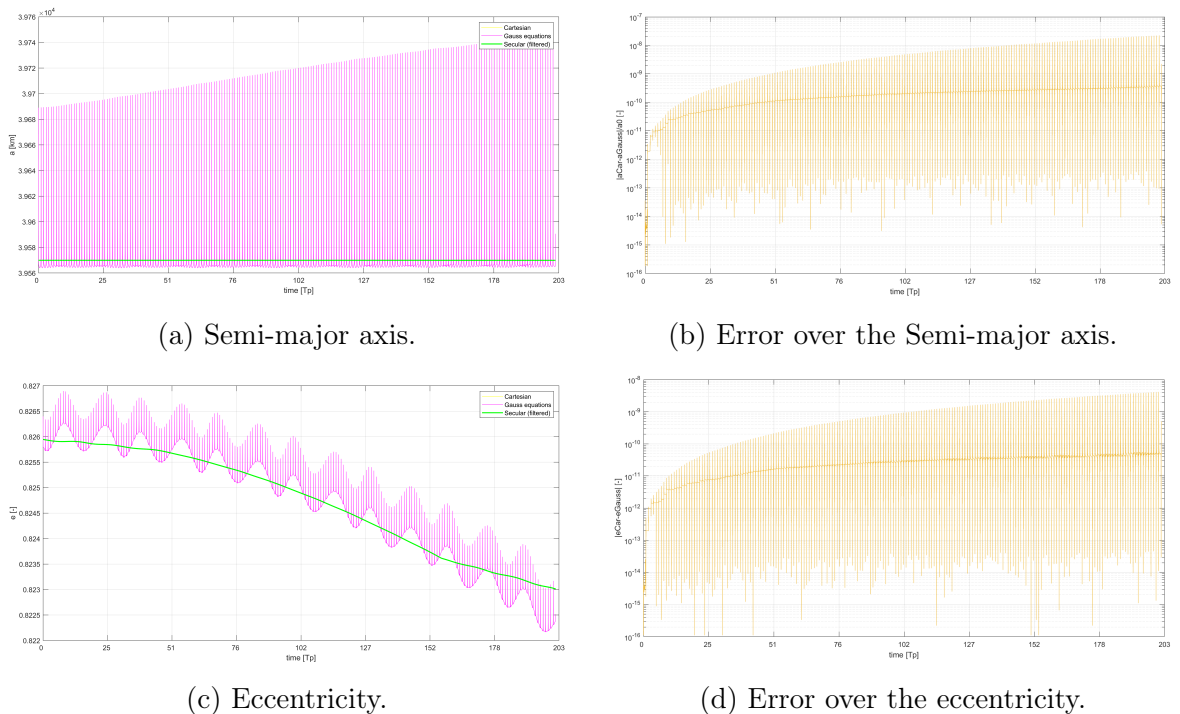


Figure 8: Keplerian elements and Relative error.

Figure 8.a shows that the semi-major axis oscillates between a minimum and a final value. On the other hand, as shown in Figure 8.c, the eccentricity initially oscillates about its initial value and then decreases keeping an oscillatory motion.

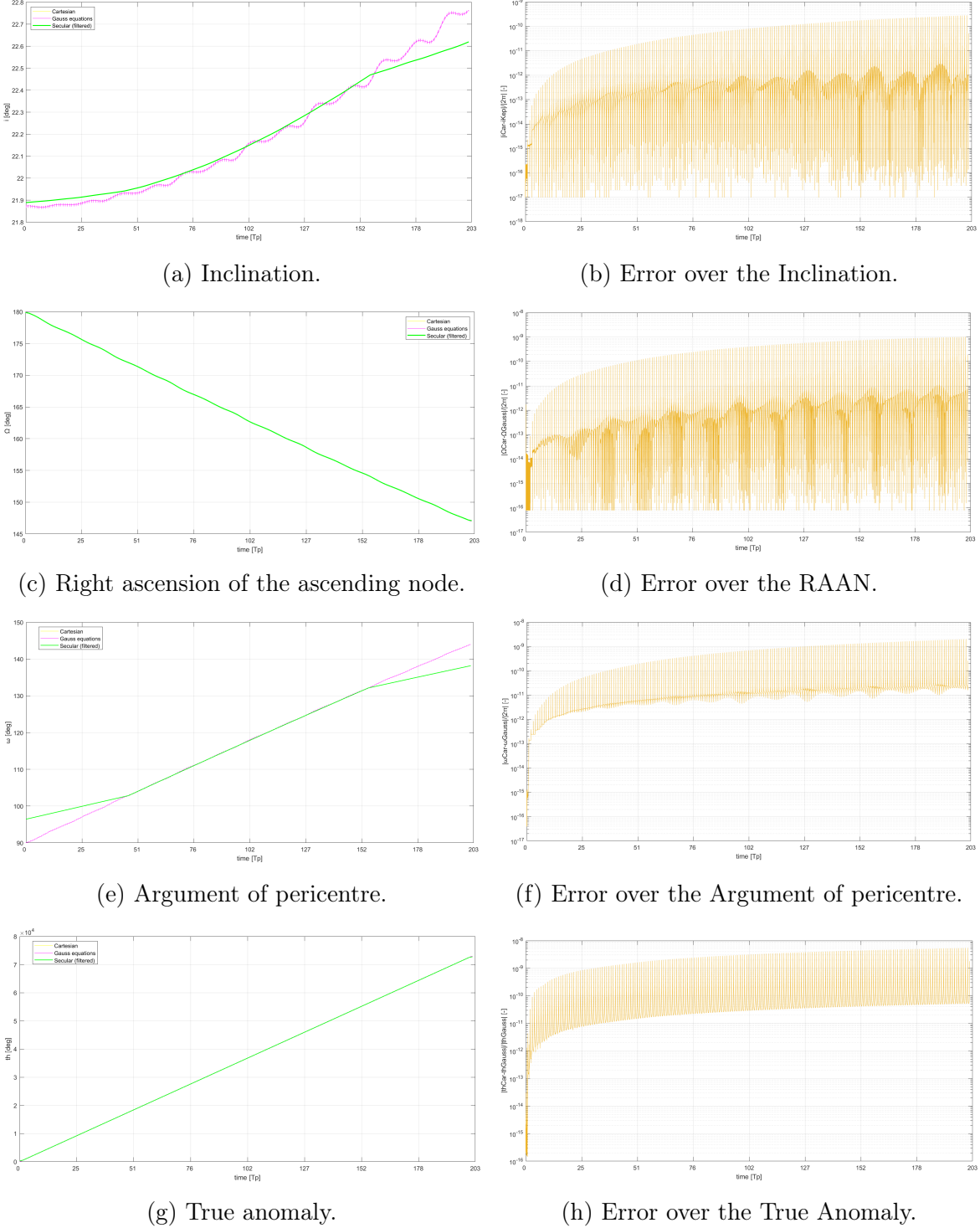


Figure 9: Keplerian elements and Relative errors.

The inclination is shown to increase over time from its initial value. In contrast to this, the RAAN decreases with time in a near linear manner. This can be observed in Figures 9.a and 9.c. Both the argument of pericentre (Figure 9.e) and the true anomaly (Figure 9.g) increase linearly over time. In the case of Figure 9.g, true anomaly data have been unwrapped before the filtering in order to avoid jumps.

All relevant values from the previously mentioned figures are presented in Table 8.

Orbital element	a [km]	e [-]	i [deg]	Ω [deg]	ω [deg]	θ [deg]
Initial value	39689	0.8264	21.8645	180	90	0
Minimum value	39564	0.8225	/	/	/	/
Final value	39744	0.8268	22.7500	147	144	360
Maximum relative error	10^{-7}	10^{-8}	10^{-9}	10^{-8}	10^{-8}	10^{-8}
Secular perturbation	/	Moon	Moon	J2	J2+Moon	J2

Table 8: Keplerian elements history data

The high frequency filtering time window depends on the main perturbation of the considered orbital element. Whenever the main perturbation is J2, the time window is set to be equal to the orbital period; whenever the main disturbance is the Moon, the time window is equal to the Sidereal month (Moon's orbital period). If there is a combination of both, a sum of the two time windows is applied.

2.6 Orbit plot

The orbit was plotted over a time period of six months; this can be observed in Figure 10 where the unperturbed orbit is highlighted in pink.

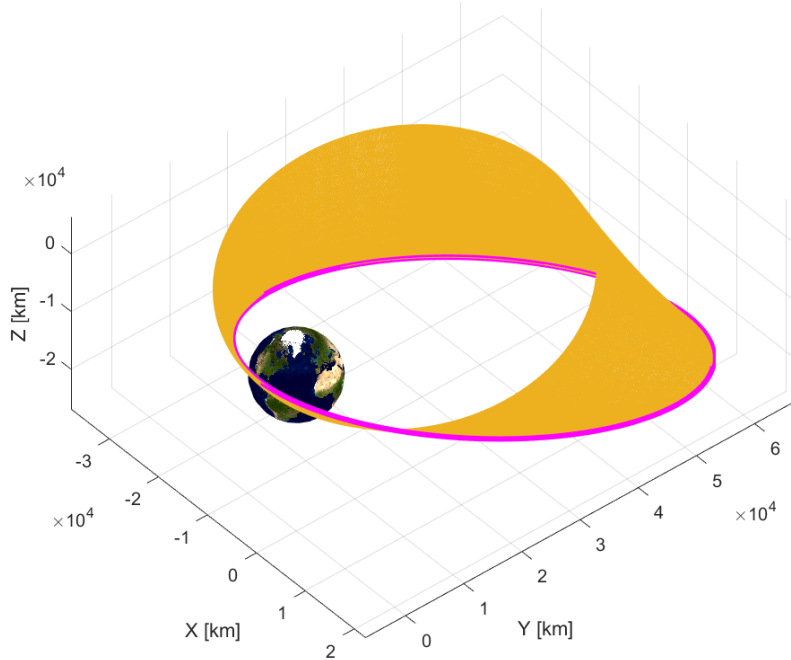


Figure 10: Perturbed orbit over six month.

2.7 Comparison with real data

To make a comparison between the propagation of the given orbit and real data, the orbit of a rocket body (DELTA 4 R/B, catalogue ID: 39169) was selected to complete the analysis.

hp [km]	ha [km]	a [km]	e [-]	i [deg]
570	65962	39644	0.8247	20.50

Table 9: Delta 4 R/B data.

The orbit of Delta 4 R/B was propagated for six years starting from the 03-08-2015 using the developed propagator and the results were compared with the data obtained from the Ephemerides [2] [3]. In the following Figure 11 are shown the behaviours of some orbital elements obtained from the propagation (in pink) and derived from the Ephemerides (in orange).

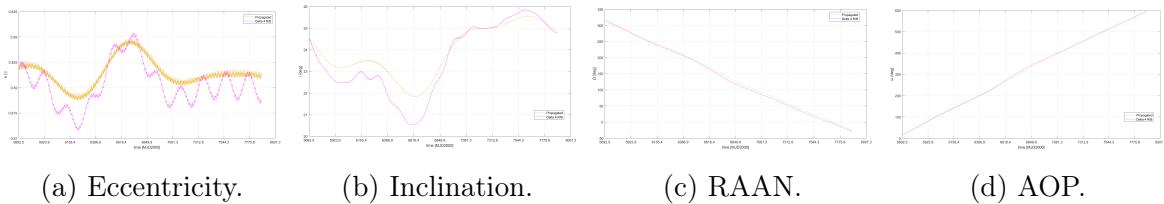


Figure 11: Comparison with real data.

2.8 Conclusions

In conclusion, the results from the planetary mission analysis show that the repeating ground tracks do not work when considering the J2 and Moon perturbation. The effect of the perturbing torques matches the theoretical estimation; this is also confirmed by the successful implementation of the high frequency filters in the selected time windows. The computational time between the propagation with the Cartesian coordinates and the Gauss's Planetary Equation is similar. The results of the comparison with the real data validates the develop propagation method.

References

- [1] Howard D. Curtis, Orbital Mechanics for Engineering Students, Elsevier, 2005.
- [2] Space-Track (2023) <https://www.space-track.org/auth/login>.
- [3] Horizons System (2023) <https://ssd.jpl.nasa.gov/horizons/app.html>.